Evidence of an Associative Intermediate on the Myoglobin Refolding Pathway

David Eliezer,* Kaori Chiba,‡ Hirotsugu Tsuruta,§ Sebastian Doniach,¶ Keith O. Hodgson,‖ and Hiroshi Kihara**
Departments of *Physics, ¶Applied Physics, and ‖Chemistry, Stanford University, Stanford, California 94305 USA; ‡Department of Biological Sciences, Tokyo Institute of Technology, Yokohama, Kanagawa, Japan; §Stanford Synchrotron Radiation Laboratory, Stanford University, Stanford, California 94309 USA; **Department of Physics, Jichi Medical School, School of Nursing, Yakushiji, Tochigi, Japan

ABSTRACT Time-resolved small-angle x-ray scattering using the stopped-flow method has been applied successfully to investigate the refolding of myoglobin. This is the only method to date that yields direct information on protein physical dimensions during the folding process. It has the potential to detect and probe important processes, such as protein compaction and association, on a millisecond time scale. Initial experiments were performed with horse myoglobin denatured in high concentrations of urea. The denatured protein was diluted rapidly into a buffer containing no urea or low concentrations of urea. The time-course of the forward-scattered intensity shows a decrease in amplitude which is clearly not engendered by the compaction of the protein, but does correspond well to a dimer dissociation process. Initial and final radii of gyration correspond well to a dimer and a monomer, respectively. Kratky plots of the initial and final states also support the transient dimerization model. The apparent dissociation rate constant was obtainable directly from the data. An association rate constant and an equilibrium constant could be estimated. The dimerizing intermediate is speculated to be a globular non-native state with an exposed hydrophobic surface.

INTRODUCTION

The search for intermediates on the protein folding pathway has been advanced by techniques such as pulsed-labeling NMR and time-resolved circular dichroism (CD) spectroscopy (for example, see Refs. 1–3). Information relating to the kinetics of secondary structure formation is obtainable now. In order to understand the forces driving the formation of the observed secondary structure and to understand its role in subsequent folding steps, it would be helpful to know the size of the protein at the times in question. However, a probe capable of measuring protein spatial dimensions during folding has been lacking.

Time-resolved small-angle x-ray scattering (SAXS), when combined with very high flux synchrotron sources, is capable of providing such physical information. Initial applications of this technique were performed using temperature as the denaturing agent and accessed a time scale of seconds (4). We describe herein a study using chemical denaturation and stopped-flow methods to investigate the refolding pathway of horse muscle myoglobin on a tens of milliseconds time scale from a physical perspective.

MATERIALS AND METHODS

Horse skeletal muscle myoglobin was purchased from Sigma Chemical Company, St. Louis, MO (crystallized and lyophilized, salt-free, 95–100% pure) and stored frozen until use. The purchased protein was not purified further. Protein samples of 60 mg/ml were prepared in 7 M urea, 50 mM bis-tris-propane buffer at pH 9.1, with salt concentrations of 100 mM NaCl and 40 mM NaCN. The presence of the cyanide was necessary to prevent potential aggregation in solutions of unfolded protein (5; K. Chiba, manuscript in preparation). The samples were allowed to equilibrate for at least 1 h before use, and were always used within 24 h of preparation in order to avoid urea decomposition. No aggregation was observed in any of the protein samples, and upon spinning at 15000 rpm for up to 1 h, no precipitate was observed. Protein-free dilution buffers were prepared at identical pH, NaCl, NaCN, and buffer concentrations, with urea concentrations of 0, 1, and 2 M; buffers were used within 24 h of preparation.

For equilibrium studies, 5 mg/ml protein samples were prepared at the same pH and salt concentrations, and at urea concentrations varying from 0 to 8 M in 1 M increments. Initially, because the need to go to subzero temperatures was anticipated, these samples also contained 40% ethylene glycol. Later, additional samples without ethylene glycol were prepared, but time constraints allowed only for experiments at 0, 1, 2, 3, and 8 M urea for these latter samples.

Measurements were made at the Photon Factory (National Laboratory for High Energy Physics, Japan) small-angle scattering beam-line 15A, where a bent-crystal horizontally focusing monochromator and a vertically focusing mirror provide a very intense beam of photons (6). The detector used was a Rigaku (Tokyo, Japan) gas-filled linear position-sensitive proportional counter. A 2.3-m sample-to-detector path length allowed collection of data in the angular range of $S = 0.002$ to 0.025 Å^{-1} (where $S = 2\sin\theta/\lambda$, 2θ is the scattering angle, and λ is the x-ray wavelength). The x-ray stopped-flow rapid-mixer, developed in collaboration with T. Nagamura and Unisoku Inc. (Hirakata, Osaka, Japan) has been described in detail elsewhere (7), and it has been employed successfully in time-resolved studies of quarternary structural changes of proteins (for example, see Ref. 8). The machine is capable of mixing small sample volumes (20–100 μl) at various mixing ratios, at a controlled temperature (±0.1°C), and with a mixing dead-time of 10 ms.[1] All time-resolved experiments were run at 8 or 15°C. Beam-line data acquisition software allowed for the collection of data in a series of discrete time-intervals or frames. Frame duration was chosen to be between 20 and 200 ms, depending on the rate of the observed process. In all cases, a total of 94 frames were collected.

All time-resolved measurements were made using a 6:1 (dilution buffer: protein solution) mixing ratio. This resulted in final urea concentrations of

Received for publication 9 December 1992 and in final form 22 April 1993.
Address reprint requests to Keith O. Hodgson.

0006-3495/93/08/912/06 $2.00

[1] We note in particular that the ability of the machine to adequately mix solutions of highly different viscosities is documented in Ref. 7 and that other investigators have successfully used Unisoku rapid mixers in similar CD experiments (3, 9).

1.0, 1.9, and 2.7 M, and in a final protein concentration of 8.6 mg/ml. Controls were performed by mixing together protein-free solutions and also by mixing protein-containing solution with identical buffer solution, so that no change in the protein environment occurred. No time-dependent signal was observed in the control data. Background data were collected immediately before or after protein data collection. Protein-free solution and dilution buffer, of the identical make-up as the following protein-containing solution and dilution buffer, were mixed and static data were collected for 300 s. Time-resolved protein data were accumulated for five mixing events at a time, and at least 10 separate accumulations were collected for each condition, for a minimum of 50 mixing events. Immediately following the time-resolved data collection, static data were measured from the mixed sample to record the final condition.

Equilibrium data were collected at 15°C in a flat 20-μm quartz window cell. The fragile windows and restricted access to the cell interior made it difficult to wash the cell between samples and introduced a small uncertainty in the urea concentrations of the samples. Exposure times were from 300 to 600 s.

ANALYSIS

Reproducibility of the time-resolved data was verified by comparing different data sets collected under the same conditions, and was excellent in all cases. Subsequently, data sets were averaged and normalized by the average incident beam intensity during the data collection. Background data were then subtracted from the protein data. The resulting data were fit to a Gaussian shape (10) using a nonlinear least-squares fitting routine in order to obtain the radius of gyration (R_g) and forward-scattered intensity (I_0) for each time-frame of data and for the static data. The data also were fit using conventional Guinier fits in the angular region of S = 0.0045–0.01 Å, and the agreement between the different fitting procedures was excellent. Examples of raw data frames and Guinier fits can be seen in Fig. 1. Statistical errors in the data were propagated correctly through the fitting procedure. I_0 showed a strong time-dependent signal. Although interparticle interference effects (10) exist at the protein concentrations used, our experience has shown them to be only a few percent in absolute magnitude, and the effects on the magnitude of changes in R_g or I_0 within the time-course of the experiments are expected to be smaller still.

Although repeated accumulation improved the statistical quality of the data, the final SAXS patterns from the 20–200-ms duration time-frames were very noisy, and time-courses of R_g could not be used. Initial state R_g values were obtained by averaging the values from the first five frames of each data set. Because the values from the different data sets were equal within the margin of experimental error, they were also averaged together. Final-state R_g values were calculated in a similar fashion, using the last 40 frames of data.

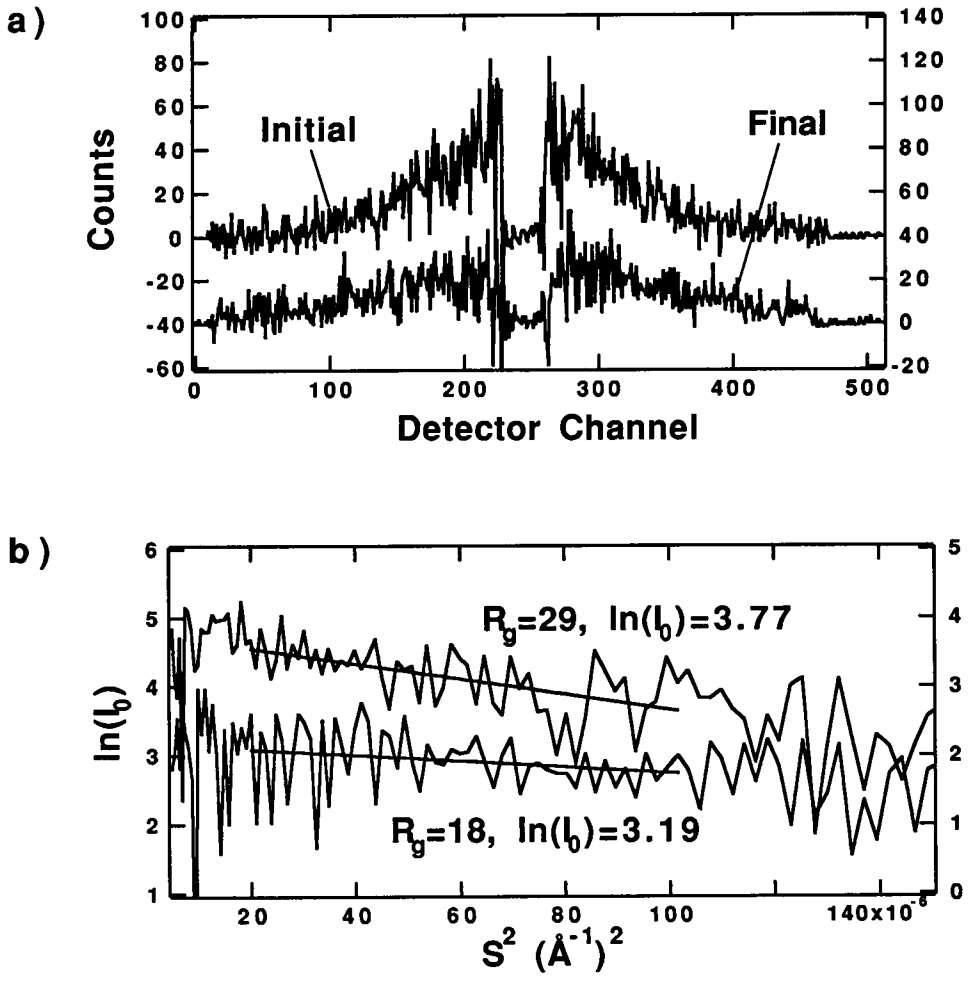

FIGURE 1 (*a*) Raw background-subtracted data for the initial and final frames of a time course. Each frame represents 100 ms of data collection averaged over 50 separate accumulations. Sample conditions were 7.0 M initial and 1.9 M final urea concentration, 0.49 mM final protein concentration and 15°C. (*b*) Guinier plots and fits to the same two frames.

Errors were propagated throughout the averaging and it was verified that the individual values that were averaged together were contained reasonably in the calculated standard deviations.

Kratky plots for the initial state were obtained by averaging time-frames over one half-life of the observed time-course in I_0. In all cases, this average was found to overlay well onto the Kratky plot for the first time-frame alone. Kratky plots for the final state were obtained in a similar fashion, using the 40 final frames, during which no time dependence was observed.

The equilibrium data were processed as above using Guinier fits to extract R_g and I_0 (Fig. 2). The R_g values at 0, 1, 2, 3, and 8 M urea were the same in the presence or absence of ethylene glycol, within the margin of experimental error. Unfortunately, only data from ethylene glycol-containing samples is available presently at the intermediate urea concentrations. The observed unfolding transaction appears to be shifted to a somewhat higher urea concentration when compared with CD data collected under identical conditions in the absence of ethylene glycol (CD data were collected on an Aviv 60DS spectropolarimeter using a 1-mm pathlength and at a 25 μM myoglobin concentration).

Despite the cursory nature of the equilibrium study, the quality of the data is sufficient to verify that much like other probes, SAXS is sensitive to unfolding transitions in proteins. This fact has also been demonstrated more thoroughly by other investigators (11). In addition, this data show that there is no apparent sample aggregation at intermediate urea concentrations.

Neglecting interparticle interference effects, the value of I_0 from SAXS data is proportional to $c(\rho_s - \rho_b)^2V^2$ (where

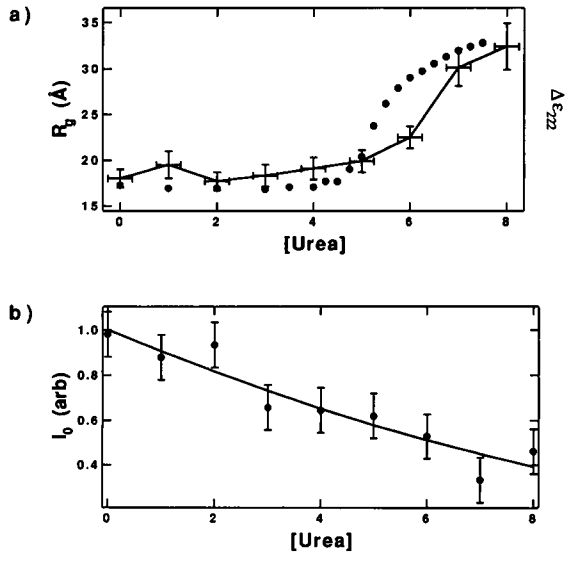

FIGURE 2 (*a*) Equilibrium melting curve of myoglobin monitored by the radius of gyration (R_g) and by the CD signal at 222 nm. The CD data have been visually scaled to the R_g data along the ordinate. (*b*) The forward scattered intensity (I_0) as a function of urea concentration. Note that the quadratic curve best fitting the data is slightly concave, as expected from the $(\rho_s - \rho_b)^2$ dependence of I_0.

c is the concentration of the scattering molecule, V its volume, ρ_s its electron density, and ρ_b is the background solvent electron density) (10). A calculation of the variation of $(\rho_s - \rho_b)^2$ with urea concentration, using 0.45, 0.33, and 0.363 $e^-/Å^3$ for the electron densities of myoglobin, water, and 8 M urea in water, respectively (11, 12), shows that I_0 should decrease by about 50% while going from 0 to 8 M urea. This agrees reasonably well with the observed decrease of I_0 in the equilibrium data (Fig. 2 *b*). The decrease, then, is caused mostly or entirely by the change in solvent density. This result implies that if the background solvent remains the same during the unfolding or refolding of myoglobin, as is the case after initial mixing in our time-resolved experiments, no change of I_0 should be observed as a result of the conformational change alone. We note additionally that we have observed I_0 to remain constant during the thermal denaturation of other proteins, where no change in background solvent takes place (unpublished results).

RESULTS

SAXS is sensitive to changes in the size, shape, and density of the scattering molecule. The time-dependent signal observed in our data must be caused by either a change in the conformation of myoglobin (refolding) or by an association or dissociation of myoglobin. In order to determine which process is responsible, we examined the R_g values, Kratky plots, and I_0 time-courses obtained from the data.

The R_g obtained from the initial time-frames (32 ± 3 Å) is consistent with that of either a small oligomer or an unfolded state, but not with that of the native state (18 ± 1 Å). The R_g from the final time-frames (20 ± 2 Å) is in good agreement with the native state value. Thus the observed change in R_g can not be used to distinguish between a monomer-refolding process and a dimer or multimer-dissociation process.

Recently, it has been shown that Kratky plots can be used to distinguish between coil-like and globular scatterers (13, 14). Kratky plots of static data from unfolded myoglobin have a shape characteristic of coil-like scatterers and different from the shape of Kratky plots of data from native myoglobin or other globular scatterers (Fig. 3). Initial time-frame Kratky plots do not show the coil-like characteristic shape of unfolded myoglobin (Fig. 4). Instead, they show a shape characteristic of a globular scatterer. This directly implies that, immediately after the mixing of the solutions, the protein is no longer an unfolded monomer. This result, together with the high initial R_g value, leads us to conclude, instead, that the sample contains small globular protein oligomers. Under the initial conditions (before mixing) and under the final conditions (after equilibrium has been reached), no aggregation is detected in the samples. Therefore, the oligomers detected in the initial frames of the experiment indicate the presence of an associative intermediate state.

After initial mixing, the background solvent remains the same throughout the ensuing measurements. As discussed above, under identical solvent conditions, I_0 of unfolded

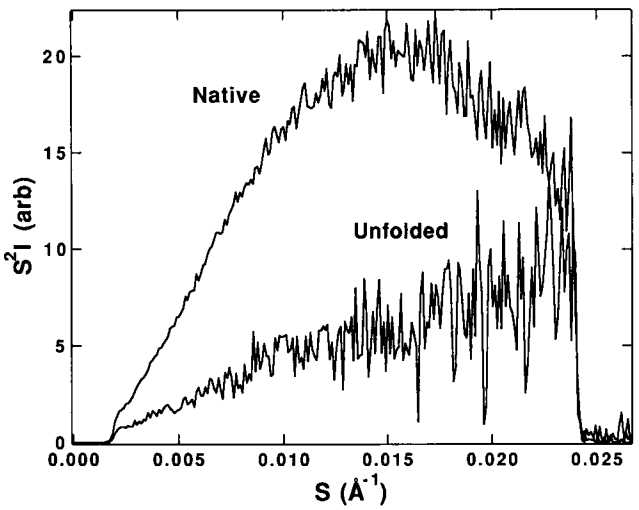

FIGURE 3 Kratky plots from urea-unfolded and native myoglobin. The broad peak in the native data indicates that the scattering molecule is compact. The persistent linear rise of the unfolded data is characteristic of a random coil molecule.

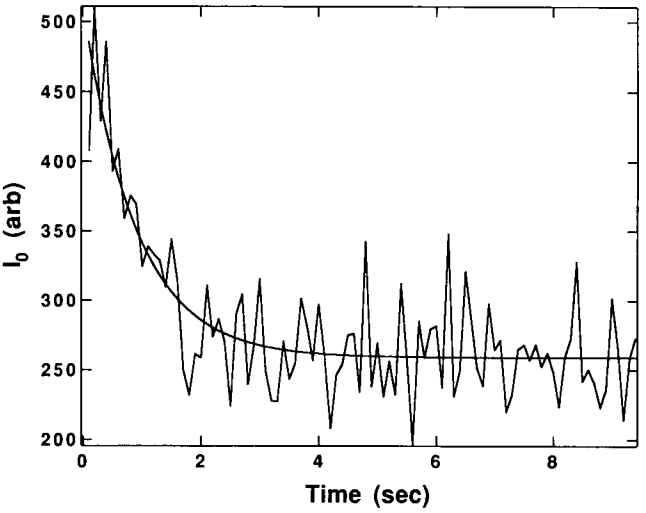

FIGURE 5 A representative plot of the forward-scattered intensity (I_0) versus time after mixing. The final urea concentration was 1.9 M and the temperature was 15°C. All other sample conditions were as in Fig. 4. The data were fit by a single exponential, giving a value of 2.09 for the ratio of the initial to the final I_0, and a decay rate constant of 1.24 s^{-1}.

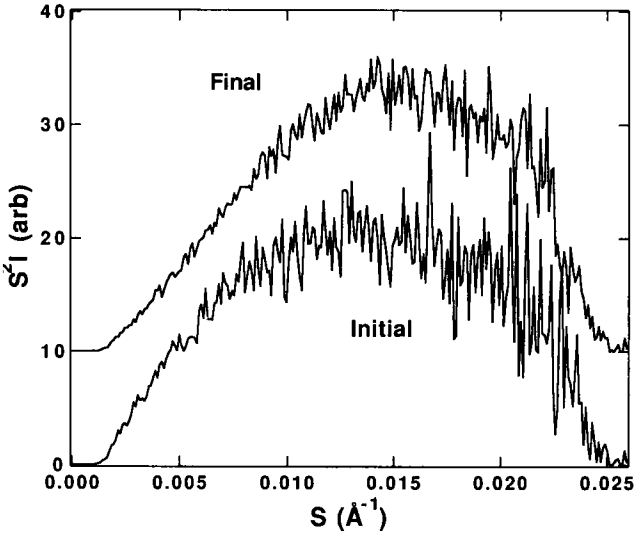

FIGURE 4 Kratky plots averaged over the first 0.8 and the last 4.4 s after mixing. The plot for the last 4.4 s has been shifted arbitrarily along the ordinate for clarity of presentation. The sample conditions were 7.0 M initial and 1.0 M final urea concentration, 0.49 mM final protein concentration and 8°C. The total exposure time was 6.9 s. The determined reaction rate constant was 0.83 s^{-1} (half-life 0.84 s). The averaged plots overlaid quite well onto the unaveraged plots of the first time-frame and last time-frame, respectively. The lack of the characteristic persistent linear rise in the initial time-frame plot indicates that the protein loses its random coil character within the mixing dead-time. The same result was observed under all other conditions.

myoglobin does not differ significantly from I_0 of the native state. Therefore, the decrease in I_0 observed in these time-resolved studies (Fig. 5) is not caused by changes in the conformation or density of protein monomers during refolding. It is most likely, then, that the decrease in I_0 is caused by a decrease in the mass of the scatterer. While solvent binding effects are well known to cause apparent mass changes in SAXS data, the change in I_0 we observe is too large to be accounted for by such effects. We conclude, in agreement with the Kratky plot analysis, that dissociation of protein oligomers is responsible for the observed decrease in I_0.

A transition from oligomer to monomer does not involve a change in electron density and, hence, the ratio of I_0 for an oligomer of n monomers to I_0 for n individual monomers is $(nV)^2/nV^2$ which is just n. Our results show that, within the rather large error margin, I_0 is always observed to decrease by a factor of about 2 (see Table 1). This leads us to hypothesize that the signal we observe in I_0 is engendered by the dissociation of the entire intermediate population from dimers to monomers. If this were the case, the concentration of dimer in the sample at any time, normalized by the initial protein concentration, would be

TABLE 1 Parameters from the time-course of the forward scattering from myoglobin during refolding

Temperature °C	Final [Urea] M	k_{app} S^{-1}	$I_0(t_i)/I_0(t_f)$
15 ± 0.1	1.0	1.91 ± .46	2.05 ± 0.23
15 ± 0.1	1.9	1.24 ± .25	2.09 ± 0.16
15 ± 0.1	2.7	0.37 ± .04	1.85 ± 0.09
8 ± 0.1	1.0	0.83 ± .11	2.22 ± 0.16

For all samples the myoglobin concentration was 3.42 mM before mixing and 0.49 mM after mixing. The initial urea concentration in all samples was 7 M. The apparent dissociation rate constant, k_{app}, and the ratio of the forward scattering at the initial and final time-frames, $I_0(t_i)$ and $I_0(t_f)$, were determined from single exponential fits to the data. Fits and errors were calculated using the program Igor (WaveMetrics, Lake Oswego, OR). Errors were correctly propagated where necessary. The ratio $I_0(t_i)/I_0(t_f)$ should be two if the protein is completely dimerized within the mixing dead-time. The decrease of k_{app} with increasing final denaturant concentration has been observed in other cases as well (3, 16).

$$\frac{[D](t)}{[M](0)} = \frac{I_0(t)/I_0(\infty) - 1}{2} \quad (1)$$

where $[D]$ represents the dimer concentration and $[M](0)$ the initial (before mixing) monomer concentration. Additional support for this hypothesis is provided by the fact that the time-course of I_0 for all samples, although noisy, is well fit by a single exponential (defining the determined rate constant to be the first order apparent dissociation rate constant, k_{app}). It is necessary to emphasize, however, that the quality of the data is not sufficient to exclude the possibility of smaller amounts of trimers and higher order oligomers, and/or of a second or higher order dissociation process.

Far from being unprecedented, our results add to the growing body of evidence that transient association may be a commonly occurring process on protein folding pathways (15–17). Most notably, bovine carbonic anhydrase B recently was shown, using high-performance liquid chromatography, to undergo a dimerization process during refolding (15).

DISCUSSION

We propose two possible folding pathways to explain our experimental results. In the first pathway, the protein undergoes a conformational change while in the dimerized state and then proceeds to dissociate and continue refolding. This pathway is represented as

$$\begin{array}{ccccc} & & \overset{k_i}{\rightarrow} & \overset{k_n}{} & \\ U & & \mathrm{I} & \rightarrow & N \\ & \overset{k_d}{\downarrow} & & & \uparrow k'_d \\ & D & \underset{k_{d^*}}{\rightarrow} & D^* & \end{array} \quad (2)$$

where U and N represent the unfolded and native state respectively, I represents the intermediate whose existence we have inferred, D represents the dimer of this intermediate, and D^* represents D after a further conformational change.

We follow the analysis in (15) and make the reasonable assumption that $k_i \gg k_d, k_n$. Under this assumption the initial concentration of I equals the initial protein concentration. Because dimerization is observed to be rapid and complete, we also assume that $k_d \gg k_n$. If the above assumptions hold, then either k_{d^*} or k'_d are rate determining in this pathway, and k_{app}, the rate constant measured for the decay of I_0, is likely to equal the lesser of these. If $k'_d \gg k_{d^*}$, then k_{app} represents the rate of conversion from D to D^*. If $k_{d^*} \gg k'_d$, then k_{app} represents the rate of dissociation of D^*.

A second proposed pathway is simpler and more closely follows that presented in Ref. 15. Here, no conformational change takes place in the dimerized state.

$$\begin{array}{ccccc} & & \overset{k_i}{\rightarrow} & \overset{k_n}{} & \\ U & & I & \rightarrow & \mathrm{N} \\ & \overset{k_d}{\Downarrow} & & & \Uparrow k'_d \\ & & \mathrm{D} & & \end{array} \quad (3)$$

We make the same assumptions about k_i and k_d as above. Then, if $k'_d \gg k_n$, D and I are in rapid equilibrium, and the transition from I to N is the rate determining step for dimer dissociation.

If, instead, $k_n \gg k'_d$, then the dimerization of the intermediate effectively increases its lifetime, the transition from D to I will be the rate-determining step for the dimer dissociation, and k_{app} equals k'_d.

Unfortunately, further information is required to discriminate between the above pathways and interpretations. We note also that other possible intermediates on the above pathways are included implicitly in U and N, because our probe is not able to distinguish among them. They are either too short-lived or they do not significantly differ in size or shape from U or N.

Because the dimerizing species is not long-lived under our conditions, we do not know its association equilibrium constant. We note, however, that this intermediate is possibly the same one detected by Phillips in a thermal denaturation study of myoglobin (4), and that therefore it may be possible to study its properties in equilibrium under those conditions, where a much longer lifetime was observed. In the meanwhile, we note that the dimerization of the protein appears to be completed within the dead-time of the rapid mixer, which is 10 ms. We use this observation to set a lower limit of about 1 ms^{-1} mM^{-1} or 10^6 s^{-1} M^{-1} for the dimerization rate constant, k_d. If we assume that the measured apparent rate constant k_{app} is actually k'_d in the second pathway above, then the equilibrium association constant $K = k_d/k'_d$ is in the vicinity of 10^6 M^{-1} under our various conditions. These values of k_d and K are similar in magnitude to values reported in the literature for similar processes in carbonic anhydrase B, bovine growth hormone, and lactate dehydrogenase (15, 16, 18). Although this similarity is encouraging, we emphasize that the numeric K value we obtained is only a rough estimate, because the presence of even a small amount of higher order oligomers or aggregates may have a significant effect on the magnitude of k_{app}.

CONCLUSION

We propose that our dimerized intermediate is globular and that much of the native myoglobin helical structure has formed. Globularity is supported by the Kratky plot analysis, and the fast formation of secondary structure has been observed in CD studies (unpublished data). We further speculate that the helices have not yet arranged themselves correctly. Because the helices are highly amphipathic, this could leave the extremely hydrophobic interior regions of the helices exposed, and interprotein helix interactions could lead to association and an accompanying stabilization of the intermediate state. A reorganization of the helices might be responsible for the ensuing dissociation. While there are many other possibilities, we find this explanation appealing because compact globular intermediates with fluctuating tertiary structure (sometimes referred to as molten-globule states) are suspected to be a common motif in protein folding pathways (19).

We believe that the demonstrated ability of time-resolved stopped-flow SAXS to measure protein size as a function of time makes it uniquely applicable to studying the processes of compaction and association during protein refolding. Although under our experimental conditions compaction probably occurred too fast to be observed, it is a necessary event in the folding pathway of every protein, and it is becoming evident that association is at least a potential event in folding pathways as well. Further applications of the method to a wider range of proteins should elucidate previously undetectable steps in their folding pathways, and provide critical constraints for future models of general protein folding pathways.

We are grateful to Dr. G. V. Semisotnov for useful discussions and to Dr. Y. Amemiya for technical assistance.

This work was supported by National Institutes of Health grant RR01209 (to K. O. Hodgson) and by a National Science Foundation graduate fellowship (to D. Eliezer.). Data were collected at the Photon Factory, National Laboratory for High Energy Physics, Japan.

REFERENCES

1. Udgaonkar, J. B., and R. L. Baldwin. 1988. NMR evidence for an early framework intermediate on the folding pathway of ribonuclease A. *Nature.* 335:694–699.
2. Roder, H., G. A. Elöve, and S. W. Englander. 1988. Structural characterization of folding intermediates in cytochrome *c* by H-exchange labelling and proton NMR. *Nature.* 335:700–704.
3. Sugawara, T., K. Kuwajima, and S. Sugai. 1991. Folding of staphylococcal nuclease A studied by equilibrium and kinetic circular dichroism spectra. *Biochemistry.* 30:2698–2706.
4. Phillips, J. C., A. D. LeGrand, and W. F. Lehnert. 1988. Protein folding observed by time-resolved synchrotron x-ray scattering. *Biophys. J.* 53:461–464.
5. Shack, J., and W. M. Clark. 1947. Metalloporphyrins VI. Cycles of changes in systems containing heme. *J. Biol. Chem.* 171:143–187.
6. Amemiya, Y., K. Wakabayashi, T. Hamanaka, T. Wakabayashi, T. Matsushita, and H. Hashizume. 1983. Design of a small-angle x-ray diffractometer using synchrotron radiation at the Photon Factory. *Nuclear Instruments and Methods.* 208:471–477.
7. Tsuruta, H., T. Nagamura, K. Kimura, Y. Igarashi, A. Kajita, Z.-X. Wang, K. Wakabayashi, Y. Amemiya, and H. Kihara. 1989. Stopped-flow apparatus for x-ray scattering at subzero temperature. *Rev. Sci. Instrum.* 60:2356–2358.
8. Tsuruta, H., T. Sano, P. Vachette, P. Tauc, M. F. Moody, K. Wakabayashi, Y. Amemiya, K. Kimura, and H. Kihara. 1990. Structural kinetics of the allosteric transition of aspartate transcarbamylase produced by physiological substrates. *FEBS Lett.* 263:66–68.
9. Kuwajima, K., H. Yamaya, S. Miwa, S. Sugai, and T. Nagamura. 1987. Rapid formation of secondary structure framework in protein folding studied by stopped-flow circular dichroism. *FEBS Lett.* 221:115–118.
10. Glatter, O., and O. Kratky. 1982. Small Angle X-ray Scattering. Academic Press, London. 515 pp.
11. Stuhrmann, H. B. 1980. Small-angle x-ray scattering of macromolecules in solution. *In* Synchrotron Radiation Research. S. Doniach and H. Winick, editors. Plenum Publishing Corp. New York. pp. 513–531.
12. CRC Handbook of Chemistry and Physics. 1987. CRC Press, Boca Raton, Florida. p. D-266.
13. Kataoka, M., Y. Hagihara, K. Mihara, and Y. Goto. 1993. Molten globule of cytochrome *c* studied by small angle x-ray scattering. *J. Mol. Biol.* 229:591–596.
14. Ramakrishnan, V., L. Patthy, and W. F. Mangel. 1991. Conformation of Lys-plasminogen and the Kringle 1–3 fragment of plasminogen analyzed by small-angle neutron scattering. *Biochemistry.* 30:3963–3969.
15. Cleland, J. L., and D. I. C. Wang. 1992. Transient association of the first intermediate during the refolding of bovine carbonic anhydrase B. *Biotechnol. Prog.* 8:97–103.
16. Brems, D. N., S. M. Plaisted, H. A. Havel, and C.-S. C. Tomich. 1988. Stabilization of an associated folding intermediate of bovine growth hormone by site-directed mutagenesis. *Proc. Natl. Acad. Sci. USA.* 85: 3367–3371.
17. Mitraki, A., and J. King. 1989. Protein folding intermediates and inclusion body formation. *Bio-Technology.* 7:690–697.
18. Kiefhaber, T., R. Rudolph, H.-H. Kohler, and J. Buchner. 1991. Protein aggregation *in vitro* and *in vivo*: a quantitative model of the kinetic competition between folding and aggregation. *Bio-Technology.* 9:825–829.
19. Ptitsyn, O. B. 1987. Protein folding: hypotheses and experiments. *J. Protein. Chem.* 6:273–293.